A Novel Ray-shooting Method to Render Night Urban Scenes
A Method based on Polar Diagrams

M. D. Robles-Ortega, J. R. Jiménez and L. Ortega
Department of Computer Science. University of Jaén, Paraje Las Lagunillas s/n, Jaén, Spain

Keywords: Polar Diagrams, Large 2.5*D* Urban Models, Hard Shadows, Ray-shooting.

Abstract: Illumination and shadows are essential to obtain realistic virtual environments. Nevertheless, large scenes like urban cities demand a huge amount of geometry that must somehow be structured or reduced in order to be manageable. In this paper we propose a novel real-time method to determine the shadowed and illuminated areas in large scenes, specially suitable for urban environments. Our approach uses the polar diagram as a tessellation plane, and a ray-casting process to obtain the visible areas. This solution derives the exact illuminated area with a high performance. Moreover, our approach is also used to determine the visible portion of the scene from a pedestrian viewpoint. As a result, we only have to render the visible part of the scene, which is considerably lower than the global scene.

1 INTRODUCTION

Shadow rendering is essential to achieve realistic images of virtual environments. In fact, it has been a prolific research line since the beginnings of the computer graphics field. Nevertheless, illumination of urban scenes with many light sources is still an open problem if the real-time rendering is pursued as a goal. The complexity and the large size of common cities is usually a challenge to obtain realistic results in interactive environments.

Nowadays the process of modeling real urban scenes is normally performed from imagery and LIDAR scans as described in (Musialski et al., 2013). Although there are also techniques that work from cadastral data (Robles-Ortega et al., 2013), as it is done in this paper. In any case the realism is obtained by means of real geometry and real facades photographs, which evidently increases the storage requirements, especially when the goal is to model entire cities. In order to simplify an urban scene, building models are usually represented as 2.5D objects in the related work (Argudo et al., 2012).

In this paper we propose a novel ray-shooting approach based on polar diagrams (Grima et al., 2006) to obtain precise direct illumination in city models. The scenes use photorealistic models located in a night urban scene and directly illuminated by a set of street lamps. Our geometric-based approach requires a very few number of rays to determine the set of illuminated areas in comparison to the classical image-based ray-casting. In a night urban scene, lampposts are mainly the light that illuminates certain portions of the buildings, the rest remains in shadow. These lighted areas can come from several sources, each of them adding intensity to each illuminated pixel depending on the distance to the light source. Our exact method works in two phases: (1) obtaining the exact visible set from the viewpoint or camera position and (2) computing shadows in this portion of the visible environment. The first phase is a ray-casting process to obtain the visible portion of scene from the viewpoint. In the second, the illuminated and shadowed areas are computed following a similar process using polar diagrams as well. In both phases, the polar diagram allows us to exploit the spatio-temporal coherence, which makes the process more efficient.

In a previous work (Robles-Ortega et al., 2009), visibility is solved in terms of buildings to accelerate walkthrough problems. In this paper we extend the method to resolve a precise direct illumination in city models. Visibility is now solved in terms of primitives by determining the specific intersection points. The processing times are comparable to those obtained by classical shadow maps and shadow volume approaches. Moreover, the storage requirements are improved because only the essential number of photographs is required for a given viewpoint, since our method obtains the exact geometry.

The paper is structured as follows. In Section 2 we

Robles-Ortega M., Jiménez J. and Ortega L..
A Novel Ray-shooting Method to Render Night Urban Scenes - A Method based on Polar Diagrams.
DOI: 10.5220/0004718800530063
In *Proceedings of the 9th International Conference on Computer Graphics Theory and Applications* (GRAPP-2014), pages 53-63
ISBN: 978-989-758-002-4

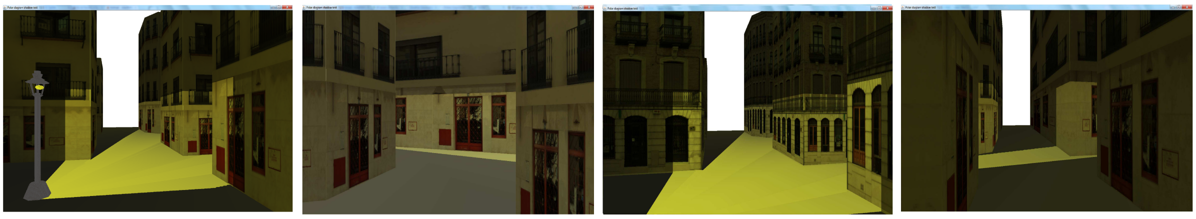

Figure 1: Sample view from a city in which it is only necessary to render a 0.1% of the total geometry.

detail the related previous work. Next, in Section 3 we define the polar diagram and its angular characteristics for visibility and shadow determination. Following, in Section 4 we detail our approach to be applied in 2.5D urban scenes. Finally, Section 5 presents our results and, Section 6 the main conclusions and the future work.

2 PREVIOUS WORK

Virtual cities have a huge amount of applications such as traffic simulation, visual impact analysis of architectural projects or computer games (Wonka and Schmalstieg, 1999). In recent years there is a growing interest in working with virtual cities. Despite real-time visualization of these environments is a very challenging problem (Cignoni et al., 2007), there is no specific bibliography for realistic rendering of large cities considering the shadows that buildings cast (Dorsey and Rushmeier, 2008).

In the literature we can find a number of algorithms for massively rendering cities such as the blockmaps (Di Benedetto et al., 2009) or the texture-atlas tree (Buchholz and Dollner, 2005). These approaches usually adapt traditional acceleration strategies (such as level of detail, image-based rendering and visibility culling techniques) to the particular properties of city models: 2.5D overall shape, plane-dominant geometry, regular structure, dense occlusion, large texture datasets (Argudo et al., 2012) or geometry simplification (Germs and Jansen, 2001).

As stated in (Revanth and Narayanan, 2012), culling approaches avoid rendering the geometry that is ultimately not visible, which is especially useful in web-client systems. Occlusion culling techniques perform particularly well in urban environments (Wonka et al., 2001), in which buildings are normally big occluders (Koldas et al., 2007). Our proposed method firstly makes a drastic geometry reduction using a novel occlusion culling method. Thanks to this approach, the data that should be processed are reduced and the GPU is released of rendering big scenes. The method is based on the polar diagram (Grima et al., 2006), which performs a plane subdivision on the city map. A similar approach used for web-based city walks in (Zara, 2006) also generates a sector division of a virtual city. However, the main drawback of this proposal is that the division must be added to the system manually.

Besides visibility culling techniques, another common strategy to reduce the size of the urban scene is modeling the buildings as 2.5D models (Bittner et al., 2005; Cohen-Or et al., 1998). Thus, the prism-shaped elements can be efficiently processed thanks to this simplification process without losing realism in the final scene.

To the best of our knowledge, classical real-time shadow approaches such as shadow maps or shadow volumes (Eisemann et al., 2011), are not focused on very large urban environments, and can be overwhelmed by the large amount of geometry to be processed. As a consequence, this kind of solutions can be useful in a second step to deal with the reduced scene (the visible portion from the pedestrian point of view). There are some strategies to minimize the impact of the excess of the geometry, like BSP, octree, etc. For instance, (Chin and Feiner, 1989) presented the first BSP solution related with the computation of shadows. They proposed the shadow volume BSP tree where each node is related with a shadow along a given plane. Each light source requires its corresponding SVBSP tree. For each tree, the number of nodes are minimized by grouping shadow areas of different polygons.

3 THE POLAR DIAGRAM

Visibility resolution is invaluable for the efficient development of shadow algorithms under the assumption that only the visible portion of scene must be rendered. The polar diagram solves visibility for 2D and 2.5D scenes as described in (Ortega and Robles-Ortega, 2013) for the general case, and in (Robles-Ortega et al., 2009) for urban scenes.

In this paper we demonstrate that the polar diagram can also be used to compute shadows using the same preprocessing. In summary, in a first phase of the process the polar diagram determines the section of visible scene from the viewpoint. Afterwards, the same tessellation determines which portions of this visible scene are illuminated or in shadow. In this second phase each light source is in fact used as viewpoint to solve the same visibility problem. Visible areas coincide with the lighted scene when the viewpoint is replaced by light sources. Boundaries delimiting the illuminated areas and those that remain in darkness are also determined with complete accuracy and efficiency. The first phase for visibility determination is fully detailed in (Ortega and Robles-Ortega, 2013). This method works with the simple 2D geometry of the building footprints, but considering the height of the buildings. It follows a ray-shooting process managing tangent lines to this two-dimensional objects. Tangent lines or bitangent lines are also referred in the literature to get the visibility complex of n convex objects in the plane (Pocchiola and Vegter, 1993). The visibility complex has also been used for radiosity computation in 2D environments (Durand et al., 1996). In this paper we focus on shadows calculation once the polar diagram has found the exact portion of visible scene.

The polar diagram associated to the scene E, $\mathcal{P}(E)$, can be defined in similar terms to the *Voronoi diagram* (Okabe et al., 1992). This tessellation finds the nearest site to a given point position in logarithmic time by locating this point in a Voronoi region. The polar diagram follows the same principle: (1) any point position p is located in the polar region of object o_i, $p \in \mathcal{P}_E(o_i)$ in logarithmic time , (2) and a winged-edge data structure speeds up ray-shooting algorithms thanks to the topological relations.

While the Voronoi diagram obtains the nearest site to a given point (Euclidean distance criterion), the polar diagram finds the nearest angular site (or polygonal object). That is, it uses the minimum angle as criterion of construction, which benefits the search of angularly close objects. The use of polar diagrams has several advantages such as being precomputed in optimal time, $\Theta(n \log n)$, and also that conservativity is ensured, which means that no visible objects are missed.

The major drawback is that no specific methods have been developed for 3D scenes. However, the extension to 2.5D scenes is straightforward. Although visibility determination is considered a complex problem in 3D scenes, urban environments have certain characteristics that make visibility to be addressable using polar diagrams. Buildings can be considered large occluders that are usually represented by prism-shaped objects, the so-called 2.5D models (Cohen-Or et al., 2003).

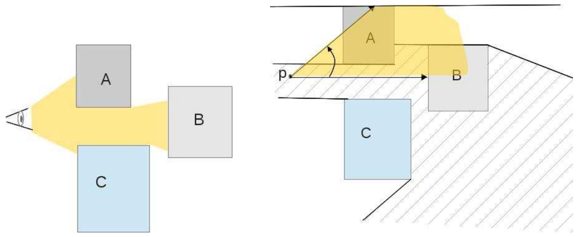

(a) Top view scene (b) $\mathcal{P}_{0+}(E)$

Figure 2: Visibility and illumination relationship.

Figure 2.a) represents the top view of a prism-shaped scene. The leftmost picture shows the portion of scene directly illuminated by a light source or directly visible by an observer. These problems can be directly solved in linear time by performing a clockwise and counterclockwise scanning from p as depicted in Figure 2.b). However, this calculation is expensive in time if the scene is very large or the observer moves. In this picture p is located in the polar region of object B. By definition of polar diagram, if $p \in \mathcal{P}_E(B)$, object B is the first visible object from p when performing an angular scanning from angle zero in counterclockwise direction, and therefore, B is visible from p. If this polar diagram works efficiently in the angular range $[0, \pi/2]$, the total angular spectrum $[0, 2\pi]$ can be covered using four polar diagrams, each of them working in a similar way for each of the four quadrants of the coordinate plane as described in (Ortega and Robles-Ortega, 2013).

Although angular proximity does not involve visibility, it identifies which are the candidates that must be checked. The resulting illuminated scene is identified by means of a ray-casting process from point p using the plane partition obtained by the polar diagram.

3.1 The Ray-casting Process

Visibility or illumination can be solved by means of a ray-casting process from the viewpoint or light source. Any ray shot $r(t)$ from p in the angular range $[0, \pi/2]$, representing a light beam, can use the $\mathcal{P}(E)$ polar diagram to determine efficiently its trajectory using the topological data structure associated to polar diagrams. If $r(t)$ intersects with object o_i, then o_i is visible from p. If a single ray can determine a visible object in a specific direction, then a fan of selected rays may determine the visible portion of the scene from p in an angular range. The view frustum is defined by the angular sector $[r_L, r_R]$, being r_L the ray defining the left side and r_R the right one. If the view frustum does not match with a quadrant, which is the usual, two or more polar diagrams will be used as described next (Ortega and Robles-Ortega, 2013):

1. Divide $[\vec{r_L}, \vec{r_R}]$ into the sub-intervals corresponding to each quadrant involved.
2. For each sub-interval $[\vec{r_l}, \vec{r_r}] \subseteq [\vec{r_L}, \vec{r_R}]$
   (a) Determine the polar diagram $\mathcal{P}(E)$ for this sub-interval.
   (b) Locate p in the polar region of object o_i, $p \in \mathcal{P}_E(o_i)$.
   (c) Determine the set of rays $R_{lr} = \{r_l, r_1, r_2, ..., r_r\}$ being for simplicity $r_j = r_j(t)$, $j \in [l, 1, 2, ..., r]$ a ray starting from the light source position p.
   (d) For each ray r_j compute a collision detection.

Of all the above steps, which deserve explanation are the collision detection process and the selection of rays. The collision detection (Step 2.(d)) is discussed in (Ortega and Feito, 2005). This process provides, the object o_v intersecting with $r(t)$ (if any). Then, o_v is visible from p and depending on the distance, o_v is directly illuminated. The algorithm describes the trajectory of $r(t)$ through adjacent polar regions until an intersection is computed or the ray leaves the scene.

The ray shooting process requires $O(N)$ time for guiding the ray $r(t)$ across the N regions of the scene. However, the worst case is very rare in dense scenes in which the ray is likely to collide with nearby objects.

Algorithm 1: Fan of tangent rays R_{lr}.

Input:

- The scene $E = \{o_1, o_2, ..., o_n\}$
- The light source position p

Output: The fan of tangent rays $R_{lr} = \{r_l, r_1, r_2, ..., r_r\}$

BEGIN

1. Let V the set of visible objects from p, $V = \emptyset$
2. Let $T = \emptyset$ a data structure of rays angularly sorted from left to right
3. Insert r_l and r_r into T
4. While T is not empty
   (a) Get and remove the first element r_i from T
   (b) Insert r_i into R_{lr}
   (c) Shoot r_i and detect the collision with object $objInt$
   (d) Determine $[r_j, r_{j+1}]$ the consecutive rays in R_{lr} such that $r_i \in [r_j, r_{j+1}]$
   (e) If $objInt \neq$ Null AND $objInt \notin V$ AND $[r_j, r_{j+1}]$ is not a closed range
      i. Insert $objInt$ into V
      ii. Insert in T the left and right tangent to object o_i
5. return R_{lr} angularly sorted

END

Next we define the *tangent ray* and *fan of tangent rays* concepts:

Definition 1. The tangent ray: *$r_i = \{p,\ ptTg,\ objTg,\ ptInt,\ objInt\}$ represents the set of attributes associated to the ray r_i, being p the origin of the ray (viewpoint), $objInt \in E$ is the object collided by r_i in the point $ptInt$, $objTg \in E$ is the object such that r_i is tangent to $objTg$ and $ptTg$ is the tangent point of r_i in $objTg$. We denote $R_{lr} = \{r_l, r_1, r_2, ..., r_r\}$ as the* ***the fan of tangent rays*** *with origin in p, angularly sorted and using a single polar diagram $\mathcal{P}(E)$.*

All these tangent rays r_i form the corresponding fan of tangent rays R_{lr} which finds exact visibility. The advantages of tangent lines are that the set R_{lr} is as reduced as possible (only $O(2k)$ rays for k visible objects). In addition light sources also follow tangent lines direction, which makes our method especially suitable for illumination purposes.

The ray-casting process described in Algorithm 1 generates a fan of rays angularly sorted from p. Each ray launched may detect a new visible object o_v which is inserted in the set V of visible objects. Then the left and right tangent lines to o_v are inserted in the set T of rays to be processed in the same way. The result is a fan of tangent rays described above defining the exact illuminated areas of the scene (see Definition 1). Each tangent ray is determined by the origin and end point of r_i, the visible object $objInt$ and its intersecting point $ptInt$, as well as the information about the tangent object $objTg$, if any, and the tangent point $ptTg$.

The algorithm follows inserting the two rays defining the view-frustum r_l and r_r in T (Step 3). r_l is the first ray angularly sorted and the first one that is shot. Whenever a launched ray r_i intersects with an object $objInt$, its left and right tangent rays are inserted in T to be processed later, but only if this new ray satisfies the following conditions:

- it is in the range $[\vec{r_l}, \vec{r_r}]$
- it does not collide with any object already inserted in V (if is not already visible)
- it is not within a *closed range* in R_{lr}.

Two neighbors rays r_j and r_{j+1}, $r_j, r_{j+1} \in R_{lr}$ provide a closed range if the angular sector $[r_j, r_{j+1}]$ only contains one object. Otherwise, the new tangent ray is inserted in T waiting to be processed in order to find new visible objects. When a tangent ray lies into a closed range or it intersects with a visible object, no additional rays are necessary to find new objects. Otherwise, r_j and r_{j+1} may contain more than one object and the algorithm must shot new tangents rays and identify which objects may be placed within $[r_j, r_{j+1}]$ (Step 4(d)).

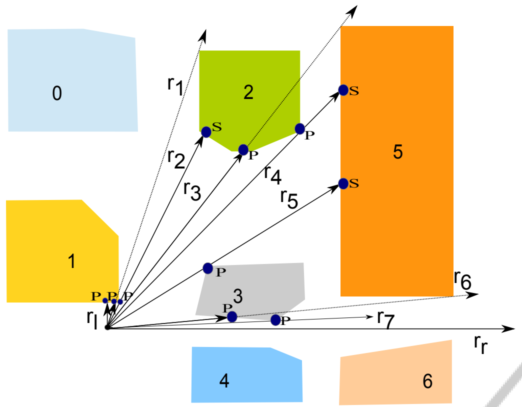

Figure 3: Fan of rays from point p.

The example of Figure 3 depicts the resulting fan of rays determining visible objects from point p after applying Algorithm 1. Initially, $T = \{r_l, r_r\}$ (Step 3), the first ray shot is r_l which collides with object o_1 (Step 3(c)). The right tangent to o_1, the ray r_2 is shot (the left one is out of range and is not considered) reaching o_2. At this point $V = \{o_1, o_2\}$ contains two visible objects. The new rays shot are r_1 and r_4, the left and right tangent rays to o_2 respectively. Among r_l, r_1 and r_2 the visible range is closed now because only one object is within each pair of these rays. The process follows when T becomes empty and V finally contains the visible set of objects.

The topological data structure of polar diagrams guides efficiently each tangent ray across the scene, and also ensures to get exactly the illuminated area. The rest of the scene remains in shadow.

Algorithm 1 shoots $O(k)$ rays to determine k visible objects, which is optimal. As each ray can cross $O(N)$ polar regions to achieve a visible object, in the worst case the fan of rays needs $O(kn)$ time for finding the visibility set. However, the illumination process is more efficient than visibility since objects cannot be illuminated beyond a specific distance. Then, illumination can be solved in $O(k)$, being k the number of illuminated objects.

4 DETERMINING THE SHADOWED AND ILLUMINATED AREAS

The fan of tangent rays determines the visible objects from the light source position, and also the frontier between their shadowed and lit areas, as described below.

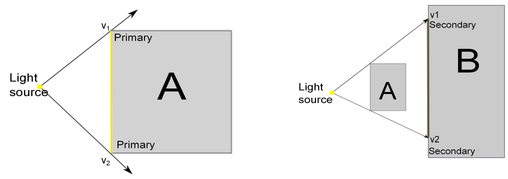

(a) Illumination from a light source. (b) Umbra points generated by two tangent rays

Figure 4: Classification of hit points.

4.1 Algorithm Details

Once the fan of tangent rays has been computed, the following step is the classification of the hit points (Definition 2) as *primary* or *secondary* points. A *hit point* is considered as primary if a tangent ray directly intersects with any other object before touching the tangent object (as points $v1$ and $v2$ in Figure 4(a)). On the contrary, if the ray hits first the tangent object before intersecting with any other in the scene, then this hit point is classified as secondary. These points are the frontier between shadowed and illuminated areas as depicted in the example of Figure 4(b). In this case, rays $r1$ and $r2$ touch object A before intersecting with B. Therefore, A casts a shadow on B, and points $v1$ and $v2$ should be considered as secondary points. The attributes of a hit point are formally described in Definition 2.

Definition 2. The hit point: $vp = \{p, obj, illuminated\}$ *represents the 2D intersecting point p between a tangent ray and the polygon obj; $illuminated$ is an attribute which classifies the point as primary when true or secondary otherwise.*

The process to determine the set of hit points from the fan of tangent rays is described in Algorithm 2. Each tangent ray is likely to intersect with any building in a hit point. These points are highly relevant in our method because they define the border between light and shadowy areas. Then, the method evaluates these hit points as primary or secondary. Specifically, there are four possible cases for each ray which are next described.

The first case (step 2a in Algorithm 2) considers the non-tangent rays r_l and r_r, defining the angular range (see Algorithm 1). These rays are the only ones that are non-tangent to any object. They may not intersect with any polygon, and then the algorithm follows with other rays. Otherwise, if the intersection is computed, the hit point is considered as primary, since there is no other object involved. This is the step 2b in the algorithm, illustrated in Figure 5.

The next case is a non-intersecting tangent ray as

Algorithm 2: Obtain and classify the hit points.

Input:

- The fan of tangent rays $R_{lr} = \{r_l, r_1, r_2, ..., r_r\}$
- The light source position p

Output: The set of hit points $S_{vp} = \{vp_1, vp_2, ..., vp_{vpn}\}$

BEGIN

1. $S_{vp} = 0$
2. For each ray r_i in R_{lr}
   (a) If r_i.ptTg is null AND r_i.ptInt is null Then continue
   (b) If r_i.ptTg=Null AND r_i.ptInt $\neq$ Null Then (Fig. 5)
      i. $S_{vp} += HitPoint(r_i$.ptInt,r_i.objInt,true);
   (c) If r_i.ptTg$\neq$Null AND r_i.ptInt=Null Then (Fig. 6)
      i. $S_{vp} += HitPoint(r_i$.ptTg,r_i.objTg,true)
   (d) If r_i.ptTg$\neq$Null AND r_i.ptInt$\neq$Null Then
      i. If (distance(lp,r_i.ptTg) $<$ distance(lp,r_i.ptInt)) Then (Fig. 7(a))
         A. $S_{vp} += HitPoint(r_i$.ptTg,r_i.objTg,true);
         B. $S_{vp} += HitPoint(r_i$.ptInt,r_i.objInt,false);
      ii. else (Fig. 7(b))
         A. $S_{vp} += HitPoint(r_i$.ptInt,r_i.objInt,true);

END

depicted in Figure 6 (step 2c). The hit point r_i.ptTg is considered as primary because there are not obstacles between object A and the light source.

There are two possible situations when a tangent ray intersects with any object (step 2d): the tangent object is in front or behind of the hit object. The first case is classified as primary like Figure 7(a) shows. In this example, object A is closer than B to the light source position. Therefore, as A casts a shadow in object B, $ptInt$ is secondary and $ptTg$ is primary. The other situation (Figure 7(b)) is the opposite because $objTg$, object B in this case, is behind the object A, which determines that $ptInt$ is primary. In this case, $ptTg$ should not be considered for classification since it is not directly illuminated from the light source.

An example of the hit points obtained using the Algorithm 2 in a full scene is shown in Figure 3. As depicted in the picture, each ray determines one or two of these intersecting points. For example, ray r_2 obtains two hit points (the first in object 1 and the second in object 2). Nevertheless, ray r_6 only includes one because the tangent point in object 5 is not reached from the light source.

4.2 Generating the Illuminated Faces of the Polygons

After classifying the hit points, the next step is determining if the polygon areas between two consecutive hit points are illuminated or shadowed (Definition 3).

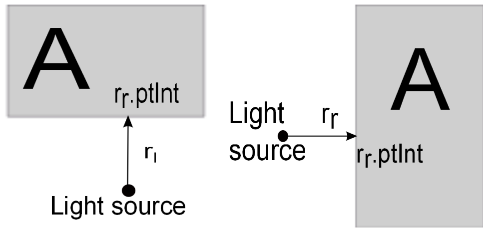

(a) r_l.ptInt is primary. (b) r_r.ptInt is primary.

Figure 5: Examples for case 2b in Algorithm 2.

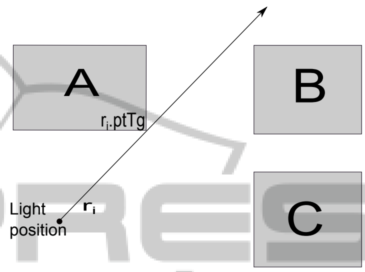

(a) Point r_i.ptTg is primary.

Figure 6: Example for case 2c in Algorithm 2.

Definition 3. The polar area: $va = \{v, illuminated\}$ *represents an interval which delimits the illuminated area of a polygon, being* $v = \{v_1, v_2, ..., v_{nv}\}$ *the set of polygon vertices delimiting the area and illuminated an attribute that classifies the area as illuminated or umbra. If illuminated is true, then the area has to be represented as lit, otherwise, it is shadowed.*

The area between two adjacent rays of the fan of tangent rays are defined as the polar area. Each of these angular sectors is illuminated or shaded, whereby each of these areas will be rendered in accordance with its classification: illuminated or umbra. The polar areas are built using the polygon vertices and the hit points, according to the process summarized in Algorithm 3. This procedure can be divided into two main parts: 1) obtaining the points which compose the area and 2) determining if they are illuminated or not.

Each area considered as illuminated or umbra is delimited by two consecutive hit points (v_i and v_{i+1}).

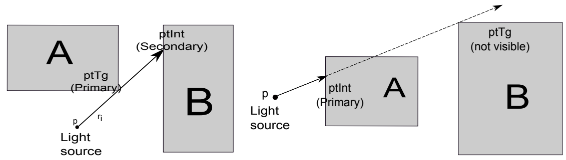

(a) r_i.ptTg is primary and r_i.ptInt is secondary. (b) r_i.ptInt is primary and r_i.ptTg is not needed as it is behind the building.

Figure 7: Examples for case 2d in Algorithm 2.

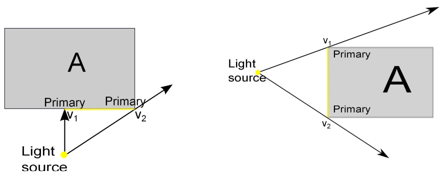

(a) Considering tangent and non-tangent rays.

(b) Only considering tangent rays.

Figure 8: Examples for case 6 in Algorithm 3.

All polygon vertices between v_i and v_{i+1} are also considered for generating the illuminated or umbra geometry in the scene. (Steps 3-5 in the algorithm).

Algorithm 3: Classify the polar areas of a polygon.

Input:

- The set of hit points $S_{vp} = \{vp_1, vp_2, ..., vp_{vpn}\}$ associated to an object o
- The vertices defining the perimeter of objects $O = \{o_1, o_2, ..., o_{on}\}$

Output: The set of polar areas of the polygon, $S_{va} = \{vp_1, vp_2, ..., vp_{van}\}$

BEGIN

For i=1 To vpn-1

1. Let be va a polar area
2. $va.v \leftarrow \emptyset$
3. $va.v$+=vp_i insert the first hit point
4. $va.v$+=O insert the rest of polygon vertices between vp_i and vp_{i+1}
5. $va.v$+=vp_{i+1} insert the last hit point
6. If (vp_i.illuminated AND vp_{i+1}.illuminated) Then
   $va.illuminated$ =True (Fig. 8)
7. If ((NOT vp_i.illuminated AND vp_{i+1}.illuminated) OR (vp_i.illuminated AND NOT vp_{i+1}.illuminated)) Then
   (a) $va.illuminated$ =true (Fig. 9)
8. If (NOT vp_i.illuminated AND NOT vp_{i+1}.illuminated) Then
   (a) If (vp_i.obj == vp_{i+1}.obj) Then
      i. $va.illuminated$ =false (Fig. 10(a))
   (b) else
      i. $va.illuminated$ =true (Fig. 10(b))

END

Once all the vertices of the polar area have been inserted, next we determine if this area is shadowed by analyzing the three possible cases of the vertices v_i and v_{i+1}:

1. If both points v_i and v_{i+1} are primary (Step 6), then the polar area is considered as illuminated. In Figure 8 the hit points determine a lit part of object A.

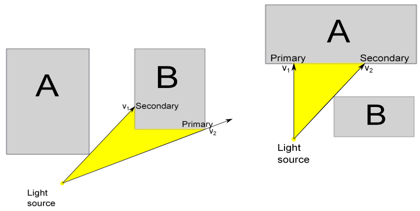

Figure 9: Examples for case 7 in Algorithm 3.

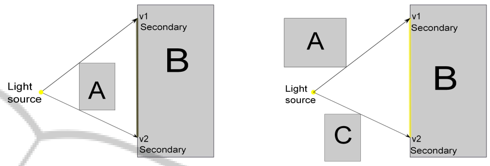

(a) Hit points are secondary, and the area between v_1 and v_2 is shadowed.

(b) Hit points are secondary, but the marked area is illuminated

Figure 10: Examples for case 8 in Algorithm 3.

2. If one of the hit point is primary and the other secondary (Step 7, Figure 9), then the area is illuminated since there are no obstacles between the light source and the object.
3. If both hit points v_i and v_{i+1} are secondary (Step 8, Figure 10) then two different cases are found depending on the object associated to the hit points:
   (a) If both hit points are generated from the same polygon, then the area is umbra. Figure 10(a) shows an example, $v1$ and $v2$ are tangent points of object A, which partially occludes the light toward polygon B.
   (b) If the hit points are tangent to different objects, as in Figure 10(b), then these points determine an illuminated area, since there are no obstacles between the light source and the object.

Figure 11 shows the polar areas of the scene of Figure 3. According to Algorithm 3, two consecutive primary points determine an illuminated area, as in the case of object 1. An example of two consecutive secondary points can be seen for object 5, however the area between them is illuminated because these two points have been generated from different objects (step 8b in the algorithm).

Finally, the polar areas are used to create the 3D model of both floor and building faces. In the first case, the illuminated parts of the floor are generated using the triangles shown in Figure 11. These triangles are built using the origin and endpoint of each polar area and the light source position. On the other hand, building faces are created by an extrusion pro-

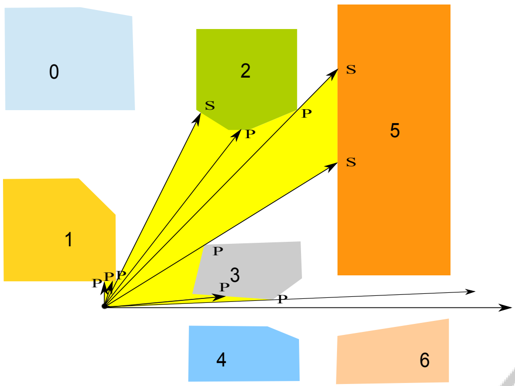

Figure 11: Determining and classifying the polar areas.

cess which uses the vertices of the polar areas.

5 RESULTS AND DISCUSSION

This section presents the tests carried out using an Intel®Core^{TM}2 Quad CPU Q2800 2.33GHz to evaluate the performance and accuracy of our method. Next we describe them in detail.

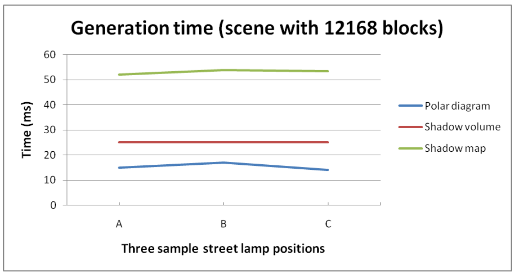

Figure 12: Generation time of three sample street lamp positions.

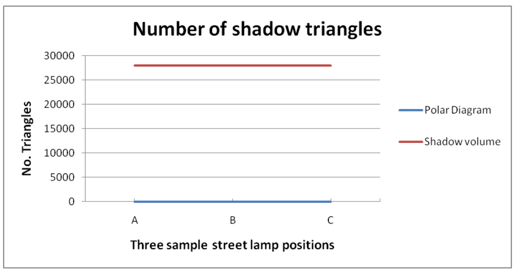

Figure 13: Number of triangles of three sample street lamp positions.

The former test compares our approach with another classical shadow techniques like shadow maps and shadow volumes with regard to performance. Specifically, two different urban scenes composed of 1183 and 12168 blocks of buildings (7.000 and 70.000 triangles respectively) have been used. For each scene, three representative street lamp positions (*A*, *B* and *C*) have been selected in different areas of the city in order to study the number of shadow triangles, and the generation and visualization time.

Table 1 summarizes the results for the polar diagram (top), shadow volume (medium), and shadow map (bottom). In the case of the polar diagram, the shadow computation time is divided into the time required to find the lit set of blocks and the ground surface. Despite this process is straightforward for shadow maps and shadow volumes, our method is faster (see Figure 12). The construction time and the visibility determination for polar diagrams can be considered as a pre-processing phase because buildings do not change and street lamps do not move during the navigation process. Therefore, these times should not be considered in the performance study.

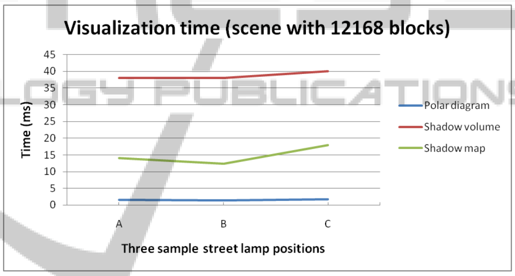

Figure 14: Visualization time of three sample street lamp positions.

Another important feature associated to our ray-casting method is its accuracy in 2.5*D* scenes, since it finds the exact set of directly illuminated primitives. As a result, the shadow geometry to be rendered in the scene is considerably reduced in comparison with the shadow volume technique which requires the generation of a significant amount of extra geometry (Eisemann et al., 2011). In our example, thousands of triangles are needed to represent the shadow volume while the polar diagram only uses dozens of polygons (see Figure 13).

Besides generation time and geometry, another important feature in performance is the visualization time. As shown in Table 1 and Figure 14, the rendering time is also more reduced for our method (on average of about 20 times). This is a direct consequence of the shadow geometry reduction since the final scene to be rendered is smaller than for the classical approaches.

In view of the results of this test, we can conclude that our method obtains a good performance in 2.5*D* scenes with regard to generation, rendering times, and geometry load. This issue is specially useful for web-based systems and low-capacity devices.

Table 1: Performance of polar diagrams, Shadow Map and Shadow Volume. Scene A(7000 triangles), Scene B(70000 triangles).

	Scene A (1183 blocks)			Scene B (12168 blocks)		
Street lamp positions (A,B,C)	A	B	C	A	B	C
Polar Diagram						
Construction time (ms)	437			1940		
No. visible buildings	1	2	2	4	2	3
Time to determine visibility (ms)	30	30	10	42	29	30
Ground shadows (No. triangles)	3	4	7	5	4	11
Ground shadows (cpu time ms)	2	1	2	13	14	13
Block shadows (No. triangles)	9	18	18	8	6	6
Block shadows (cpu time ms)	1	1	1	2	3	1
Visualization (time ms)	1	1	1	1.5	1.33	1.67
Shadow Volume						
No. vertices	9464	9464	9464	56000	56000	56000
No. Quads	2366	2366	2366	14000	14000	14000
Shadow generation (No. triangles)	4732	4732	4732	28000	28000	28000
Shadow generation (cpu time ms)	10	10	9.5	25	25	25
Visualization (time ms)	6	8	7	38	38	40
Shadow Map						
Shadow generation (cpu time ms)	14	14	13	52	54	53.5
Visualization (time ms)	6	8	7	14	12.3	18

The main purpose of the latter test is studying the behaviour of our method during a free walkthrough navigation (see four sample screenshots of this process in Figure 1). Specifically, the navigation process has been evaluated at five positions as reflected in Table 2. These results show how the number of triangles has considerably been reduced, the system manages less than 100 triangles instead of the 70.000 from the original scene. Therefore we obtain an important reduction representing the 0,14% of the global scene geometry.

With regards to graphical results, Figure 15 shows the same urban scene with different kind of illuminations. The first image (Figure 15(a)) depicts the scene after disabling all sources of light. The second image (Figure 15(b)) considers the same night scene with local illumination from a single light source without shadows. Finally, the last image shows the night scene with local illumination and the shadows generated by our method.

Another important advantage of our method is the reduced amount of memory needed to store the polar diagram structure. As Table 3 shows, the four polar diagrams only take up 175.125 bytes. This value is significantly low considering the high capacity of the current computers, and the benefits obtained by our approach described above. The table details the memory requirements for each one of the polar diagram components: polar axis (border lines between polar regions), polar regions, polygons of the scene, and the rest of fields of the data structure.

Table 2: Results for navigation using Polar Diagrams.

Position	A	B	C	D	E
No. visible buildings	5	2	3	2	2
No. Building triangles	60	24	42	18	36
No. Ground triangles	30	12	21	9	18
Generation time (ms)	14	9	9	9	9
Visualization time (ms)	1	1	1	1	1

Table 3: Memory requirements (in bytes) for polar diagrams.

	East+	East-	West-	West+	*Total*
Polar axis	7,031	6,563	7,031	6,563	27,188
Polar regions	21,5	19,938	20,75	21,063	83,25
Polygons	11,969	11,969	11,969	11,969	47,875
Rest of fields	4,063	4,063	4,344	4,344	16,813
Total	44,563	42,531	44,094	43,938	**175,125**

6 CONCLUSIONS AND FUTURE WORK

In this paper we have proposed a novel real-time method based on polar diagrams to navigate through night large virtual cities. The main strength of this

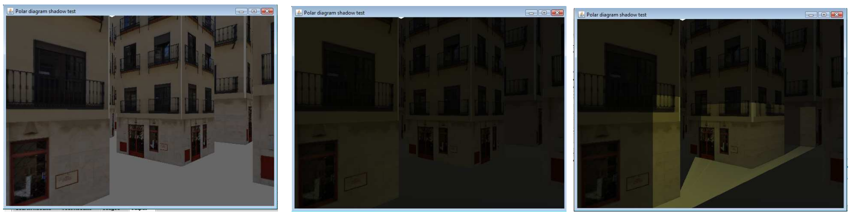

(a) No lighted scene (b) Night scene. Local illumination without shadows (c) Night scene. Local illumination and shadows generated using our method

Figure 15: Visual results.

method is the minimization of the geometry to be rendered for a given position, independently of the size of the scene. This feature makes this ray-casting method suitable to be used for lighting large urban environments in web-based systems or low-capacity devices. In view of the results, for 2.5D urban scenes, our visualization times have outperformed those obtained by classical methods like shadow maps and shadow volumes. Moreover, as our algorithm is independent of the screen resolution it is guaranteed the maximum quality with different kind of devices and without any additional geometry processing.

For future work we also consider to implement the proposed algorithms in the GPU by using OpenCL or WebCL. In our opinion we would take advantage of parallelizing the ray-casting process as well as the polar diagram construction. Furthermore, we want to extend our method to deal with mobile light sources since the topological relationships associated to polar diagrams enable the extension of this problem, as well as for navigation (Robles-Ortega et al., 2009). We think it is possible to obtain good results with a low extra cost.

As this paper is focused on urban scenes, the buildings remain static during the whole process. However, we plan to study the cost of a dynamic updating of the polar diagram. This scenario could be useful in other 2.5 environments.

In addition, as it has been shown, once the polar diagram has been generated, the computation of the illumination region from a new light source is achieved in real time. This outcome evinces the possibility of extending, in a future work, the current proposal to indirect illumination based on virtual point lights, for instance.

Another possible extension is the use of area light sources in order to generate soft shadows. The polar diagram give us a good understanding of the neighborhood and, intrinsically, it is not limited to point light sources. In that case, the portion of the area light source, visible from a given position, should be somehow determined.

ACKNOWLEDGEMENTS

This work has been partially granted by the Conserjería de Innovación, Ciencia y Empresa of the Junta de Andalucía, under the research project `P07-TIC-02773`.

REFERENCES

Argudo, O., Andújar, C., and Patow, G. (2012). Interactive rendering of urban models with global illumination. In *Computer Graphics International*, Bournemouth University, United Kingdom.

Bittner, J., Wonka, P., and Wimmer, M. (2005). Fast exact from-region visibility in urban scenes. In Bala, K. and Dutr, P., editors, *Rendering Techniques 2005 (Proceedings Eurographics Symposium on Rendering)*, pages 223–230. Eurographics, Eurographics Association.

Buchholz, H. and Dollner, J. (2005). View-dependent rendering of multiresolution texture-atlases. In *Visualization, 2005. VIS 05. IEEE*, pages 215–222.

Chin, N. and Feiner, S. (1989). Near real-time shadow generation using bsp trees. *ACM SIGGRAPH Computer Graphics*, 23(3):99–106.

Cignoni, P., Di Benedetto, M., Ganovelli, F., Gobbetti, E., Marton, F., and Scopigno, R. (2007). Ray-casted blockmaps for large urban models visualization. *Computer Graphics Forum*, 26(3):405–413.

Cohen-Or, D., Chrysanthou, Y., Silva, C., and Durand, F. (2003). A survey of visibility for walkthrough applications. *Visualization and Computer Graphics, IEEE Transactions on*, 9(3):412 – 431.

Cohen-Or, D., Fibich, G., Halperin, D., and Zadicario, E. (1998). Conservative visibility and strong occlusion for viewpace partitioning of densely occluded scenes. In *EUROGRAPHICS'98*, volume 17, pages 243–253.

Di Benedetto, M., Cignoni, P., Ganovelli, F., Gobbetti, E., Marton, F., and Scopigno, R. (2009). Interactive remote exploration of massive cityscapes. In *The 10th International Symposium on Virtual Reality, Archaeology and Cultural Heritage VAST (2009)*, pages 9–16. Eurographics.

Dorsey, J. and Rushmeier, H. (2008). Light and materials in virtual cities. In *ACM SIGGRAPH 2008 classes*, SIGGRAPH '08, pages 8:1–8:4, New York, NY, USA. ACM.

Durand, F., Orti, R., Rivière, S., and Puech, C. (1996). Radiosity in flatland made visibly simple: using the visibility complex for lighting simulation of dynamic scenes in flatland. In *Proceedings of the twelfth annual symposium on Computational geometry*, SCG '96, pages 511–512, New York, NY, USA. ACM.

Eisemann, E., Schwarz, M., Assarsson, U., and Wimmer, M. (2011). *Real Time Shadows*. A K Peters/CRC Press.

Germs, R. and Jansen, F. W. (2001). Geometric simplification for efficient occlusion culling in urban scenes. In *Proc. of WSCG 2001*, pages 291–298.

Grima, C. I., Marquez, A., and Ortega, L. (2006). A new 2d tessellation for angle problems: The polar diagram. *Computational Geometry. Theory and Applications*, 34(2):58 – 74.

Koldas, G., Isler, V., and Lau, R. W. H. (2007). Six degrees of freedom incremental occlusion horizon culling method for urban environments. In *ADVANCES IN VISUAL COMPUTING, PT I*, volume 4841 of *Lecture Notes in Computer Science*, pages 792–803.

Musialski, P., Wonka, P., Aliaga, D. G., Wimmer, M., van Gool, L., and Purgathofer, W. (2013). A Survey of Urban Reconstruction. *Computer Graphics Forum*, Early View.

Okabe, A., Boots, B., and Sugihara, K. (1992). *Spatial Tessellations: Concepts and Applications of Voronoi Diagrams*. John Wiley and Sons.

Ortega, L. and Feito, F. (2005). Collision detection using polar diagrams. *Computer & Graphics*, 29(5):726–737.

Ortega, L. and Robles-Ortega, M. D. (2013). Applied mathematics & information sciences. *ACM Trans. Graph.*, pages 1651–1669.

Pocchiola, M. and Vegter, G. (1993). The visibility complex. In *Proceedings of the ninth annual symposium on Computational geometry*, SCG '93, pages 328–337, New York, NY, USA. ACM.

Revanth, N. R. and Narayanan, P. J. (2012). Distributed massive model rendering. In *Proceedings of the Eighth Indian Conference on Computer Vision, Graphics and Image Processing*, ICVGIP '12, pages 42:1–42:8. ACM.

Robles-Ortega, M., Ortega, L., Coelho, A., Feito, F., and de Sousa, A. (2013). Automatic street surface modeling for web-based urban information systems. *Journal of Urban Planning and Development*, 139(1):40–48.

Robles-Ortega, M. D., Ortega, L., and Feito, F. (2009). An exact occlusion culling method for navigation in virtual architectural environments. In *Proceedings of the IV Iberoamerican Symposium in Computer Graphics*, pages 23–32.

Wonka, P. and Schmalstieg, D. (1999). Occluder shadows for fast walkthroughs of urban environments. *Computer Graphics Forum*, 18(3):51–60.

Wonka, P., Wimmer, M., and Sillion, F. (2001). Instant visibility. *Computer Graphics Forum*, 20(3):C411+. 22nd Annual Conference of the European-Association-for-Computer-Graphis, MANCHESTER, ENGLAND, SEP 04-07, 2001.

Zara, J. (2006). Web-based historical city walks: advances and bottlenecks. *Presence: Teleoper. Virtual Environ.*, 15(3):262–277.